

FABRICATION AND PERFORMANCE OF SUPERCONDUCTING QUARTER-WAVELENGTH RESONATORS FOR SRILAC

K. Suda*, O. Kamigaito, K. Ozeki, N. Sakamoto, Y. Watanabe, K. Yamada
RIKEN Nishina Center, Wako, Japan

E. Kako, H. Nakai, H. Sakai, K. Umemori, KEK, Tsukuba, Japan

H. Hara, A. Miyamoto, K. Sennyu, T. Yanagisawa

Mitsubishi Heavy Industries Machinery Systems, Ltd. (MHI-MS), Kobe, Japan

Abstract

A new superconducting booster linac (SRILAC) at the RIKEN heavy-ion linac is under construction. Ten 73-MHz low-beta quarter-wavelength resonators (QWRs) that operate at 4 K have been fabricated from pure niobium sheets. The cavity parts were assembled by electron beam welding. The resonant frequency for each cavity was adjusted by changing the lengths of the straight sections before welding. The performance and frequency were evaluated by vertical tests. All the cavities exceeded the design specifications of $Q_0 = 1 \times 10^9$ and $E_{\text{acc}} = 6.8$ MV/m. Details of the fabrication and frequency tuning as well as the performance of the cavities are reported.

INTRODUCTION

The RIKEN heavy-ion linac (RILAC), consisted of normal conducting cavities [1–3], was used to accelerate intense ion beams to synthesize super-heavy elements Nh [4]. RILAC is undergoing an upgrade to allow further investigations of super heavy elements and production of radioactive isotopes. The acceleration voltage of RILAC will be increased by introducing a superconducting booster linac (SRILAC). The SRILAC has ten quarter-wavelength resonators (QWRs) made of bulk niobium (Nb) contained in three cryomodules. The construction status has been presented in Ref. [5,6]. The tuning range of the tuning system used for cold operation is relatively narrow compared to the frequency change during the fabrication, polishing, pumping, and cooling processes. Therefore, to ensure that all the cavities operate at the design frequency, the frequency of each cavity must be tuned precisely during the fabrication and surface preparation processes based on a frequency tuning table. Frequency data were obtained by a low power test in the fabrication process and by a vertical test at a low temperature of 4.2 K.

DESIGN OF CAVITY

Table 1 summarizes the design parameters for the cavities [6]. The cavities was optimized for the acceleration of low β ions in c.w. mode. The RF properties were designed using the 3D simulation code of the CST Studio Suite [7]. A gap voltage of 1.2 MV is produced with a wall loss of 8 W at an operating temperature of 4.5 K. Frequency tuning during cold operation is performed by decreasing the length of each beam gap using a ‘dynamic tuner’. The tuning range

is from 0 to –14 kHz, and the tuning sensitivity $\Delta f/\Delta x$ is –18.7 kHz, where Δf is the frequency shift and Δx is the distance between the flanges of two beam ports (Fig. 1). For a maximum tuning of –14 kHz, each beam port experiences a force of 7.52 kN in the direction of the beam axis into the cavity, and the displacement of the beam port is 0.374 mm. The sensitivity for the displacement is 20.1 kN/mm. The stiffness of the cavity against helium pressure $\Delta f/\Delta p$ is –1.91 Hz/mbar (Fig. 1).

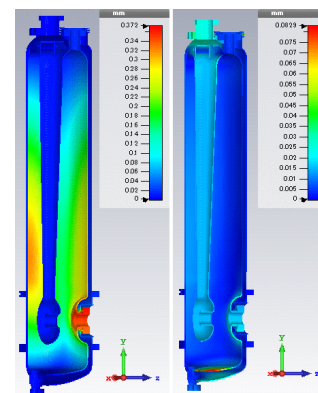


Figure 1: Simulation results for cavity at low temperature. Deformation by a force of 7.5 kN at each beam port in the direction of the beam axis (left panel) and by a pressure of 1 atm on the walls of the cavity and jacket (right panel) are shown.

Table 1: Design Parameters for Superconducting QWR

Parameter	Value
Frequency	73.0 MHz
Duty	100%
β_{opt}	0.078
Inner diameter	300 mm
Height	1097 mm
Aperture	40 mm
$G = Q_0 \cdot R_s$	22.4 Ω
R_{sh}/Q_0	579 Ω
Q_0	1.0×10^9
P_0	8 W
E_{acc}	6.75 MV/m
$E_{\text{peak}}/E_{\text{acc}}$	6.2
$B_{\text{peak}}/E_{\text{acc}}$	9.6 mT/(MV/m)

* ksuda@ribf.riken.jp

FABRICATION

Partitioning of the cavity was optimized by considering the welding process (Fig. 2), which is similar to that for the 75.5-MHz prototype cavity [8] except for a reduction of the number of ports from nine to six [6]. The major parts were made from pure Nb sheets provided Tokyo Denkai Co., Ltd. (TD) with thicknesses of 3.5 mm and 4.0 mm and a residual resistance ratio (RRR) of 250, and were shaped by press-forming. The other parts were shaped from bulk Nb by machinery. Pure Nb for the port pipes (RRR 250) and grade-2 hard Nb for the port flanges and stiffening ribs were provided by TD and ULVAC, respectively. The formed parts were combined by electron beam welding (EBW) into four sections, the top torus, stem, outer conductor, and bottom dome. Three further EBW processes were used to combine these parts together (Fig. 3). First, EBW1 welded the inner truck of the top torus and stem. Then, EBW2 welded the outer truck of the top torus and the upper part of the outer conductor. Finally, EBW3 welded the lower part of the outer conductor and the bottom dome. All the parts had short margins in straight sections for frequency tuning during fabrication. Before EBW1 and EBW3, RF measurements were performed to determine the cutting lengths of the straight sections, based on a frequency tuning table.

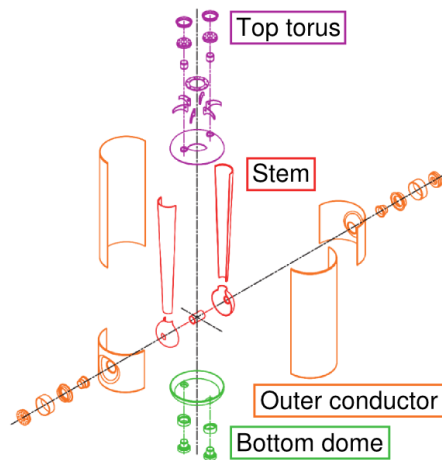


Figure 2: Division of parts.

Frequency Tuning Table

A detailed frequency tuning table was created for each cavity, according to the lecture given by M. Kelly in 2013 [9]. The tuning table for MRQ-01, the first cavity of the production type for SRILAC, is shown in Table 2. While the table starts at the design frequency of 73 MHz (#0: Cavity is cold during operation), the actual process and time sequence goes in the opposite direction, from the bottom (#20) to the top. Δf shows the change in frequency caused by each process along the table from top to bottom. Note that the sign of Δf is reversed along the time sequence. The initial table was composed of estimated and measured values for the prototype cavities. However, during the fabrication process, Δf and the frequencies were updated to the measured data

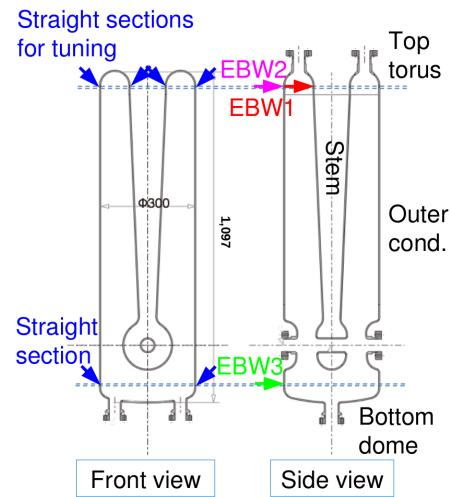


Figure 3: Straight sections of cavity (left panel) and locations of three EBW processes (right panel).

for MRQ-01. The values in parentheses are expected values for future operations. The sequence from #20 to #15 corresponds to the cutting of the straight sections and the welding processes. Δf for #20 and #17 in this tuning process, as well as that in #2 in the cooling process, were deduced from the simulation. Then, surface treatments based on a fairly standard procedure were performed in #14 to #12 [6]. Up to #12, the acceleration gaps were reduced to the design value by elastic deformation for RF measurements; however, the jigs used could not be applied in the subsequent cooling tests. Therefore, #11 shows a frequency shift due to an increase in the gaps. In the pumping and cooling processes (#10 to #8), the summed value of Δf is shown since these processes were not distinguished. The frequency data in #7 and #6 were obtained by a vertical test for the bare cavity. In #5, pre-tuning of the bare cavity was performed before jacketing, which will be described in a later subsection. After jacketing (#4) and attaching the fundamental power coupler (FPC), the cavity was assembled in a cryomodule [6, 10]. The pressure from the helium refrigerator causes a frequency shift (#2), and the dynamic tuner reduces the cavity frequency to the design value (#1).

RF Measurement by Clamping Divided Parts

In the first RF measurement, the four parts of the cavity were clamped together (Fig. 4). In order to improve RF contact and to obtain accurate results: (1) The cavity was set upside down so that the stem was pulled down against the top torus. After installing the outer conductor, the bottom dome was placed on the outer conductor and pressed down until stable frequency and Q-value data were obtained. (2) Indium wires of 1-mm diameter were clamped between all the parts. Before the measurement, the sum of the lengths of the two acceleration gaps were larger than the design value by around 0.2 mm. To adjust the gap length for the RF measurements, the beam port flanges were pressed so that the distance between the beam port flanges was reduced to

Content from this work may be used under the terms of the CC BY 3.0 licence (© 2019). Any distribution of this work must maintain attribution to the author(s), title of the work, publisher, and DOI.

Table 2: Frequency Tuning Table for MRQ-01. Δf is the change in frequency caused by each process. Δf and the frequencies are measured values unless otherwise indicated. The values in parentheses are expected values for future operations. The Δf values with (*1) are estimated by the simulation and that with (*2) is the sum of #8, #9, and #10.

#	Fabrication, polishing, pumping, cooling processes	Δf (kHz)	Frequency (kHz)
0	Cavity is cold during operation ($E_{acc} = 6.8$ MV/m at $T = 4.5$ K)	-	(73 000.000)
1	Dynamic tuner frequency shift (14 kHz at maximum)	(0.765)	(73 000.765)
2	Lower helium pressure from 0.13 to 0.1 MPa	0.573(*1)	(73 001.338)
3	Remove FPC	1.453	73 002.791
4	Remove helium jacket	4.649	73 007.440
5	Undo pre-tuning by beam port (plastic deformation)	8.702	73 016.142
6	Cavity frequency cold in vertical test ($E_{acc} = 6.8$ MV/m at $T = 4.2$ K)	-	73 016.142
7	Gap voltage 1.2 MV to 0 MV in vertical test	0.039	73 016.180
8	Warm cavity up to room temperature (4.2 K to 293 K)		
9	Vent RF space from vacuum to 0.1 MPa	-136.037(*2)	
10	Frequency shift due to dielectric constant of air (1 atm)		72 880.444
11	Redo tuning by beam port (elastic deformation)	-4.067	72 876.377
12	Add back BCP of cavity surface (BCP2: 18.2 μm)	-7.484	72 868.893
13	Undo annealing (750°C, 3 h)	-2.346	72 866.547
14	Add back BCP of cavity surface (BCP1: 114.3 μm)	-26.688	72 839.859
15	Add weld shrinkage for bottom dome (0.737 mm)		
16	Add gap between center conductor and bottom dome (0.0175 mm)		
17	Add back cut of the straight section of bottom dome (6.038 mm)	40.609(*1)	72 876.047
18	Add weld shrinkage for center/outer conductors and top torus (0.7 mm)		
19	Add indium wire clamping center/outer conductor and top torus (0.4 mm)		
20	Add back center/outer conductor cuts (10.918/10.097 mm)	-598.077(*1)	72 213.256

320.5 mm at room temperature (RT), which corresponds to the design value of 320 mm at 4.2 K. The temperature of the cavity was also measured and was used to correct the frequency to that at a temperature of 293 K for normalization.

For the second measurement after EBW1 and EBW2, the outer conductor and bottom dome were clamped without using indium wire because a good RF contact was obtained just by pressing the bottom dome.

Frequency Tuning by Adjusting Straight Sections

As mentioned above, frequency tuning was performed by adjusting the straight sections of the cavity. The cutting lengths for the straight sections were determined by the measured frequency and sensitivity obtained by the simulation. The parameters used for MRQ-01 are summarized in Table 3. There are two sensitivities for the coarse tuning: (1) stem and outer conductor, and (2) stem only. Sensitivity (2) is higher than (1) by 14%, and was used when the cutting lengths for the stem and outer conductor were different, in order to align a drift tube and end drift tubes. The alignment of the drift tube was checked before welding the bottom dome (EBW3) by inserting an MC nylon shaft ($\phi 39.4$) into the drift tubes. The change in frequency Δf_{calc} was estimated by multiplying the sensitivity and the cutting length. On the other hand, Δf_{meas} is the actual difference, where the small contributions of the weld shrinkage and indium wire thicknesses were subtracted using the sensitivities. The deviation ($\Delta f_{meas} - \Delta f_{calc}$) in Table 3 shows that the error for the fine

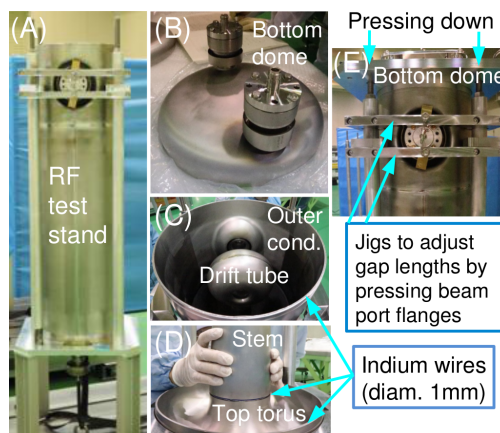


Figure 4: RF measurement by clamping the four parts together. (A) RF test stand. (B) Bottom dome. (C) Outer conductor and stem (drift tubes). (D) Stem clamped against top torus. Indium wires were clamped between the parts. (E) Bottom dome placed on outer conductor and pressed down until stable data were obtained. The jigs for adjusting the two acceleration gaps are also shown.

tuning by the bottom dome is larger than that for the coarse tuning. In order to compensate for this error, the thickness of BCP1 was reduced from the initial value of 130 μm to 110 μm for seven cavities. Although revised sensitivities between -5.2 to -5.3 kHz/mm were used for better estimation for the last three cavities, the thickness of BCP1 was kept

Table 3: Parameters for Frequency Tuning at Straight Sections

Straight section	Tuning	Sensitivity (kHz/mm)	Cutting length (mm)	Δf_{calc} (kHz)	$\Delta f_{\text{calc}}^{\text{sum}}$ (kHz)	Welding	$\Delta f_{\text{meas}}^{(*1)}$ (kHz)	Deviation (kHz)
Stem and outer conductor	Coarse	54.2	10.097	547.257	598.077	EBW1 & EBW2	603.2	5.1
Stem only	Coarse	61.9	0.821	50.820		EBW2		
Bottom dome	Fine	-6.73	6.034	-40.609	←	EBW3	-31.1	9.5

(*1) Contributions of weld shrinkage and indium wire thicknesses were subtracted using calculated sensitivities.

at 110 μm because conditions for the polishing were well established for the reduced thickness and no deterioration of the cavity performance was observed.

The error for the fine tuning was due to the position dependence of the sensitivity. Figure 5 shows the sensitivities at the straight sections of the top torus and the bottom dome. The straight sections had excess lengths of a few millimeters, and the coefficient of the sensitivity against the length is 3.1 times larger for the bottom dome than the top torus. Therefore, for the fine tuning, the sensitivity for the length before cutting should have been used instead of that at the design length.

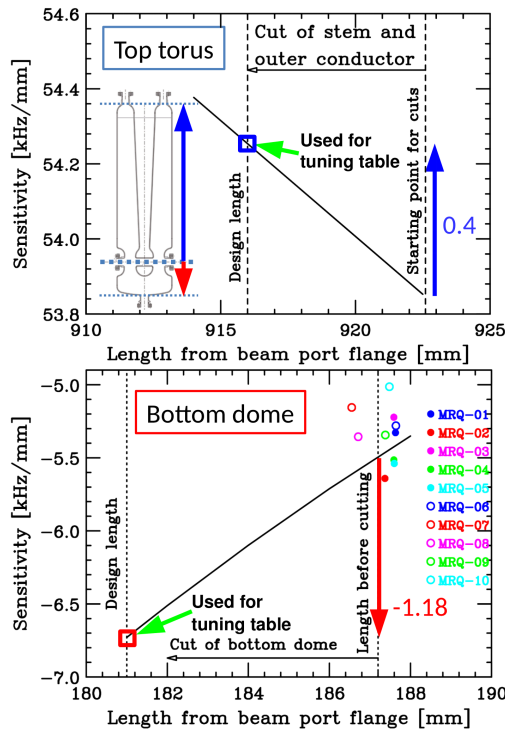


Figure 5: Tuning sensitivities at the straight sections of the top torus (upper panel) and the bottom dome (lower panel). The solid lines show the simulation results and the circles show the measured data.

Vertical Test and Performance of Cavity

The performance of the cavities was tested using the vertical test stand constructed at the RIKEN campus [5, 6, 11]. The results for bare cavities are shown in Fig. 6. The unloaded Q-factors Q_0 for all the cavities exceeded the goal at

an acceleration gradient of $E_{\text{acc}} = 6.8 \text{ MV/m}$ with no field emission. However, after jacketing, two of the four cavities

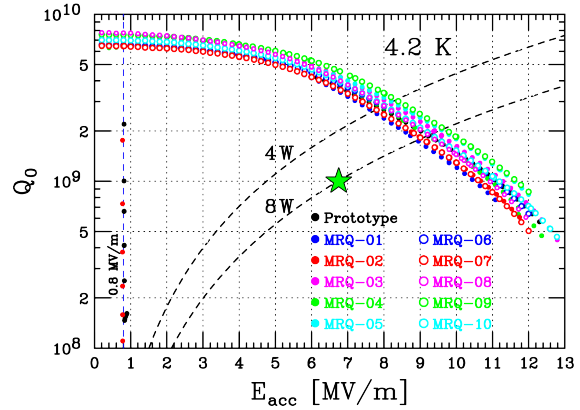


Figure 6: Results of vertical tests for bare cavities at 4.2 K. Q_0 plotted as function of E_{acc} . The green star shows the goal of the SRILAC.

showed serious field emission (Fig. 7). These deteriorations seemed to be caused by particulates entering during a slow leak procedure in the clean room at RIKEN, which was required to exchange vacuum flanges before jacketing [6]. To remove the particulates, high pressure rinsing and baking at 120°C for 48 h were performed for the two cavities. For the other six cavities, the performance after jacketing was not tested due to restrictions of the construction schedule. Therefore, the same surface treatment was carried out because of the possibility of particulate contamination.

Frequency Tuning before Jacketing

Following the vertical test on a bare cavity, the frequency was tuned by plastic deformation around the beam port at RT and 1 atm. This process was performed before welding a rigid titanium jacket using the same jigs used for gap adjustment (see Fig. 4 (E)). Figure 8 shows the tuning result for MRQ-06. In one cycle, each beam port flange was pressed by two M8 bolts (pitch of 1.25 mm) and then released. The cycle was repeated, increasing the rotation angle of the bolts by steps of 60° or 30° until the cavity was plastically deformed. Typically, 240° was sufficient for tuning.

Frequency data for the ten cavities are shown in Fig. 9. Based on the frequency of the bare cavities at 4.2 K, the required frequency change by plastic deformation was determined. The target was 73009.1 kHz, taking into account the

Content from this work may be used under the terms of the CC BY 3.0 licence (© 2019). Any distribution of this work must maintain attribution to the author(s), title of the work, publisher, and DOI.

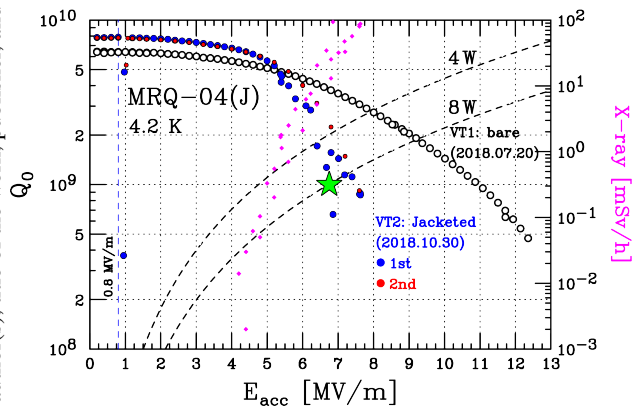


Figure 7: Performance test for jacketed cavity of MRQ-04, which had serious field emission. The level of X-rays is shown by purple circles, and was measured near the beam axis. The results for the bare cavity are also plotted for comparison.

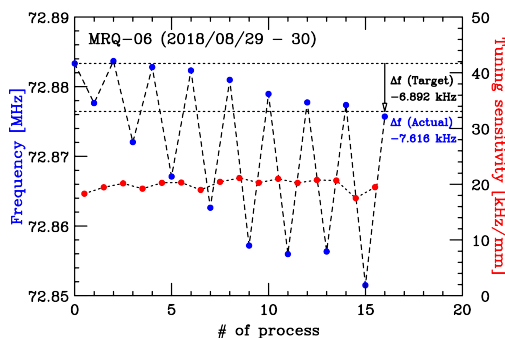


Figure 8: Frequency tuning by plastic deformation for MRQ-06.

remaining processes in the frequency tuning table. The tuning by plastic deformation was effective, though the effects of jacketing were larger than expected by ~ 4 kHz except for MRQ-03. Although the frequency decreased due to the large jacketing effect, the frequency was still in the range of the dynamic tuner.

TEST OF DYNAMIC TUNER

The dynamic tuner for SRILAC has an improved design with reduced mechanical loss in the driving system compared with the original design developed for the 75.5-MHz prototype cavity [10]. The mechanism was designed to press the beam ports by pulling surrounding wires around the cavity. Operation tests at RT and 1 atm were successfully performed, as shown in Fig. 10.

SUMMARY AND PERSPECTIVE

Ten QWRs for SRILAC have been fabricated successfully. The frequency of each cavity was tuned during fabrication based on a detailed frequency tuning table. The cavity performances exceeded the design specifications in vertical tests. A cooling test of the cryomodules is scheduled for September 2019.

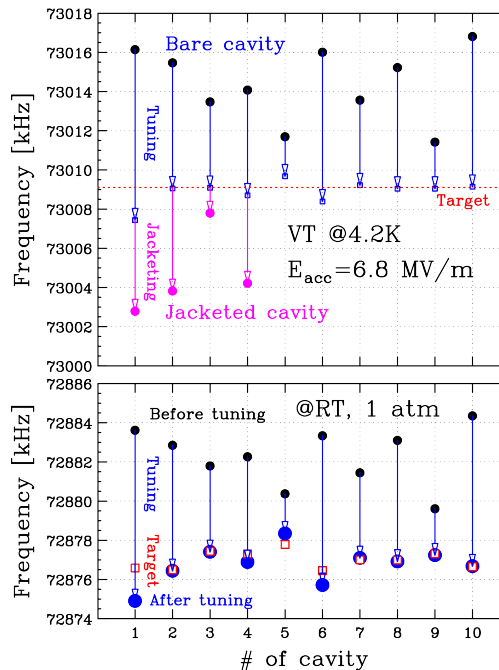


Figure 9: Frequency change by plastic deformation and jacketing. The upper panel shows the measured data at 4.2 K for the bare and jacketed cavity. The lower panel shows the data at RT before and after plastic deformation.

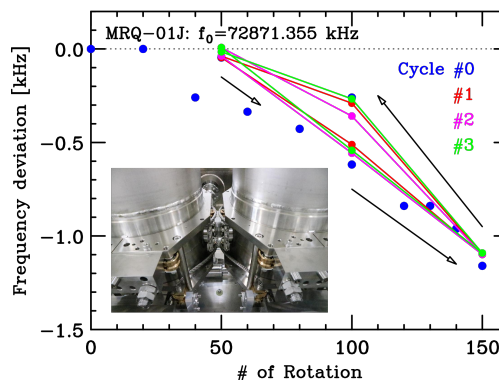


Figure 10: Test results for dynamic tuner for SRILAC.

ACKNOWLEDGEMENTS

The authors are grateful to the ImPACT Program of the Japan Council for Science, Technology, and Innovation (Cabinet Office, Government of Japan), which supported the development of the first superconducting cavity at RIKEN. The authors are also grateful to Dr. A. Kasugai at QST Rokkasho and Prof. K. Saito at FRIB/MSU for their valuable advice on the design of the cavity and on assembly work of the cryomodules.

REFERENCES

[1] M. Odera *et al.*, “Variable frequency heavy-ion linac, RILAC: I. Design, construction and operation of its accelerating structure”, *Nucl. Instr. Meth. Sec. A*, vol. 227, pp. 187–195, 1984.

- [2] O. Kamigaito *et al.*, “Construction of a variable-frequency radio-frequency quadrupole linac for the RIKEN heavy-ion linac”, *Rev. Sci. Instr.*, vol. 70, pp. 4523–4531, 1999.
- [3] O. Kamigaito *et al.*, “Construction of a booster linac for the RIKEN heavy-ion linac”, *Rev. Sci. Instr.*, vol. 76, p. 013306, 2005.
- [4] K. Morita *et al.*, “Experiment on the Synthesis of Element 113 in the Reaction $^{209}\text{Bi}(^{70}\text{Zn},n)^{278}113$ ”, *J. Phys. Soc. Jpn.*, vol. 73, pp. 2593–2596, 2004.
- [5] N. Sakamoto *et al.*, “Construction Status of the Superconducting Linac at the RIKEN Radioactive Isotope Beam Facility”, in *Proc. LINAC’18*, Beijing, China, Sep. 2018, pp. 620–625, doi: 10.18429/JACoW-LINAC2018-WE2A03
- [6] K. Yamada *et al.*, “Construction of Superconducting LINAC Booster for Heavy-Ion LINAC at RIKEN Nishina Center”, presented at the SRF’19, Dresden, Germany, Jun.-Jul. 2019, paper TUP037, this conference.
- [7] <http://www.cst.com>
- [8] N. Sakamoto *et al.*, “Construction and Performance Tests of Prototype Quarter-wave Resonator and its Cryomodule at RIKEN”, in *Proc. SRF2017*, Lanzhou, China, July 2017, doi: 10.18429/JACoW-SRF2017-WEYA02
- [9] M. Kelly, “TEM-class Cavity Design”, in *SRF’13 tutorials*, Caen, France, Sep. 2013, slide p. 61.
- [10] N. Sakamoto *et al.*, “Development of Superconducting Quarter-Wave Resonator and Cryomodule for Low-Beta Ion Accelerators at RIKEN Radioactive Isotope Beam Factory”, presented at the SRF’19, Dresden, Germany, Jun.-Jul. 2019, paper WETEB1, this conference.
- [11] O. Kamigaito *et al.*, “Measurement of Mechanical Vibration of SRILAC Cavities”, presented at the SRF’19, Dresden, Germany, Jun.-Jul. 2019, paper TUP042, this conference.